Plant Physiology, March 1999, Vol. 119, pp. 1073–1082, www.plantphysiol.org © 1999 American Society of Plant Physiologists

Impacts of Aluminum on the Cytoskeleton of the Maize Root Apex. Short-Term Effects on the Distal Part of the Transition Zone[1]

Mayandi Sivaguru[2,3], František Baluška[2], Dieter Volkmann, Hubert H. Felle, and Walter J. Horst*

Department of Plant Sciences, School of Biological Sciences, Madurai Kamaraj University, Madurai 625–021, India (M.S.); Institute of Plant Nutrition, University of Hannover, Herrenhäuserstrasse 2 D-30419, Hannover, Germany (M.S., W.J.H.); Institute of Botany, Department of Plant Cell Biology, Rheinische Friedrich-Wilhelms University of Bonn, Kirschallee 1, D-53115 Bonn, Germany (F.B., D.V.); Institute of Botany, Slovak Academy of Sciences, SK-842 23 Bratislava, Slovakia (F.B.); and Institute of General Botany and Plant Physiology, Justus Liebig University of Giessen, Senckenbergstrasse 17–21, D-35390 Giessen, Germany (H.H.F.)

Using monoclonal tubulin and actin antibodies, Al-mediated alterations to microtubules (MTs) and actin microfilaments (MFs) were shown to be most prominent in cells of the distal part of the transition zone (DTZ) of an Al-sensitive maize (*Zea mays* L.) cultivar. An early response to Al (1 h, 90 μM) was the depletion of MTs in cells of the DTZ, specifically in the outermost cortical cell file. However, no prominent changes to the MT cytoskeleton were found in elongating cells treated with Al for 1 h in spite of severe inhibition of root elongation. Al-induced early alterations to actin MFs were less dramatic and consisted of increased actin fluorescence of partially disintegrated MF arrays in cells of the DTZ. These tissue- and development-specific alterations to the cytoskeleton were preceded by and/or coincided with Al-induced depolarization of the plasma membrane and with callose formation, particularly in the outer cortex cells of the DTZ. Longer Al supplies (>6 h) led to progressive enhancements of lesions to the MT cytoskeleton in the epidermis and two to three outer cortex cell files. Our data show that the cytoskeleton in the cells of the DTZ is especially sensitive to Al, consistent with the recently proposed specific Al sensitivity of this unique, apical maize root zone.

Although evidence is increasing that the root apex plays a major role in Al perception and response (for recent reviews, see Delhaize and Ryan, 1995; Kochian, 1995; Taylor, 1995), the mechanism of Al-induced growth inhibition remains poorly understood and controversial. Whereas evidence has been shown that Al enters the root symplast in considerable quantities and possibly influences growth from the cytosolic side (Lazof et al., 1994), Horst (1995) and Rengel (1996) focused their attention on the apoplast. Recent findings on the cell wall-PM-cytoskeleton continuum (Wyatt and Carpita, 1993; Miller et al., 1997) call for a reassessment of this debate. In maize (*Zea mays* L.), detailed information on the arrangement of CMTs and actin MFs was presented for growing and developing cells of intact roots under diverse experimental conditions (Baluška et al., 1992, 1993a, 1993b, 1995, 1996a, 1996c, 1997; Blancaflor and Hasenstein, 1993, 1995a, 1995b, 1997; Baluška and Hasenstein, 1997).

More than 10 years ago, MacDonald et al. (1987) reported that Al directly influenced tubulin polymerization in vitro. Alterations of cellular growth processes by Al often induce swellings of root apices and root-hair tips (Jones et al., 1995). This phenomenon has been attributed to interactions of Al with the cytoskeleton, supposedly interfering with its structure and function (Delhaize and Ryan, 1995; Jones and Kochian, 1995). Until now, the effects of Al on the plant cytoskeleton have rarely been investigated. Alfano et al. (1993) studied the long-term effect of Al on the actin MFs in *Riccia fluitans*. Grabski and Schindler (1995), using a novel "cell optical displacement technique," reported that exposure of plant cells to Al increased the stability of actin MFs in suspension-cultured soybean cells; and Sasaki et al. (1997) reported an Al-induced depolymerization of MTs in wheat cells. Recently, Blancaflor et al. (1998) have studied Al-induced effects on MTs and actin MFs in elongating cells of maize root apices, and related the Al-induced growth inhibition to the stabilization of MTs in the central elongation zone.

Root morphogenesis is closely related to the MT cytoskeleton (Barlow and Parker, 1996), whereas the onset of root-cell elongation is thought to be actomyosin dependent

[1] This work was supported by a grant from the German Research Foundation (DFG) to W.J.H. and M.S., and also from an Indo (Ministry of Human Resource Development, Government of India)-German postdoctoral fellowship awarded by the German Academic Exchange Services, Bonn, to M.S. Partial support to F.B. was provided by VEGA (project no. 3009) of the Slovak Academy of Sciences.

[2] These authors contributed equally to this work.

[3] Present address: Japanese Society for Promotion of Science (JSPS) Postdoctoral Fellow, Research Institute for Bioresources, Okayama University, Chuo 2–20–1, Kurashiki, 710–0046, Japan.

* Corresponding author; e-mail horst@mbox.pflern.uni-hannover.de; fax 49–511–7623611.

Abbreviations: CMT, cortical MT; DFT, distance from root tip; DIC, differential interference contrast; DTZ, distal part of the transition zone; MF, microfilament; MT, microtubule; NPA, *N-1*-naphthylphthalamic acid; PM, plasma membrane; TZ, transition zone.

(Baluška et al., 1996b, 1997). Moreover, radial versus longitudinal expansion of cells within root apices is well known to be controlled by phytohormonal (auxin, GA, and ethylene) interactions with the cytoskeletal elements (for review, see Shibaoka, 1994; Baluška et al., 1998). With respect to these growth determinants, Al apparently interacts directly and/or indirectly with factors that influence the organization of the cytoskeleton, such as levels of cytosolic Ca^{2+} (Jones et al., 1998), Mg^{2+}, and calmodulin (Haug, 1994; Grabski et al., 1998), cell-surface electrical potential (Kinraide et al., 1992; Papernik and Kochian, 1997; Takabatake and Shimmen, 1997), callose formation (Horst et al., 1997), and lipid composition of the PM (Zhang et al., 1997).

Based on the previous characterization of Al toxicity in maize roots (Ryan et al., 1993), we have recently identified the DTZ as the most Al-sensitive apical root zone in the Al-sensitive maize cv Lixis (Sivaguru and Horst, 1998). In the present study we extend the characterization of this zone, which apparently plays a major role in the expression of Al toxicity in the maize root apex. We show that Al-induced inhibition of root growth is closely related to impairments of electrical properties of the PM, of callose formation, and of the structural integrity of cytoskeletal elements, specifically in cells of the DTZ. These findings provide circumstantial evidence that the DTZ represents a potential target root zone with respect to Al toxicity.

MATERIALS AND METHODS

Plant Material, Growth Conditions, and Experimental Treatments

Seeds of maize (*Zea mays* L. cv Lixis), which have been classified as Al-sensitive (Llugany et al., 1994; Horst et al., 1997), were soaked for 8 h and germinated in moistened rolls of filter paper. The rolls were positioned vertically in a growth chamber and kept under controlled environmental conditions with 70% RH, 30°C and 25°C day and night temperatures, and 300 μmol m^{-2} s^{-2} photon flux density for 16 h per day. Uniform seedlings, with root lengths ranging from 4 to 5 cm, were selected after 3 d and transferred to aerated nutrient solution with the following composition (in μM): $CaSO_4$, 250; KNO_3, 400; $MgSO_4$, 100; Fe EDDHA, 20; $MnSO_4$, 1; $ZnSO_4$, 0.1; $CuSO_4$, 0.2; KH_2PO_4, 10; H_3BO_3, 8; $(NH_4)_6Mo_7O_{24}$, 0.1; and NH_4NO_3, 200 (pH 4.3). The seedlings were transferred to fresh nutrient solution after 24 h, and 300 μM Al from a stock solution, prepared from an Al atomic spectroscopy standard solution ($AlCl_3 \cdot 6 H_2O$, 1000 mg L^{-1}, Fluka), was added to a nutrient solution to achieve a final monomeric Al concentration of 90 μM (measured using the aluminon technique according to the method of Kerven et al. [1989]).

Fixation, Embedding, and Sectioning

Apical root segments (10 mm) of primary root apices from control (untreated) and experimental seedlings were excised into 5 mL of stabilizing buffer (50 mM Pipes, 5 mM EGTA, and 5 mM $MgSO_4$, pH 6.9) containing 5% DMSO for 15 min at room temperature. Afterward, they were fixed with 4% paraformaldehyde in a stabilizing buffer containing 10% DMSO for 60 min at 20°C. Alternatively, root apices were excised and fixed with 3.7% formaldehyde in the stabilizing buffer for 60 min at room temperature for visualizing F-actin arrays. After a brief rinse in the stabilizing buffer, they were dehydrated in a graded ethanol series diluted with PBS (pH 7.1). The Steedman's wax was prepared by mixing 9 parts of PEG 400 distearate (Aldrich) and 1 part (w/w) of 1-hexadecanol (Aldrich), as reported earlier (Baluška et al., 1992, and refs. therein). Root segments were infiltrated with the mixtures of absolute ethanol and wax, made up in the proportions 2:1, 1:1, and 1:2 (v/v) for 2 h (37°C) at each step. Followed by three changes in pure wax under a vacuum, the infiltrated roots were embedded in pure wax and allowed to polymerize at room temperature. From the embedded material, 8-μm-thick longitudinal sections were made. Intact ribbons of median sections were allowed to expand on a drop of de-ionized water and mounted on slides coated with glycerol-albumen (Serva, Heidelberg, Germany).

Immunofluorescence Localization of MTs

The mounted sections were dried at room temperature overnight. Then they were dewaxed in ethanol, rehydrated in an ethanol/PBS series, and allowed to stand in a stabilizing buffer for 45 min. To facilitate tubulin-antibody penetration, sections were digested with an enzymatic mixture (1% hemicellulase [from *Aspergillus niger*, Sigma-Aldrich], 0.5 M EGTA, 0.4 M mannitol, 1% Triton X-100, and 0.3 mM PMSF, all dissolved in a stabilizing buffer) for 15 min. The digestion reaction was terminated by transferring the slides to the stabilizing buffer for 15 min followed by 1% Triton X-100 in a stabilizing buffer for 10 min. After a brief rinse in stabilizing buffer, sections were incubated with mouse monoclonal antibody raised against chick brain α-tubulin (Amersham), diluted 1:200 in PBS for 60 min at room temperature in darkness. Following a further rinse with a stabilizing buffer, the sections were stained with fluorescein isothiocyanate-conjugated anti-mouse IgG raised in goat (Sigma), diluted 1:200 in PBS for 60 min at room temperature in darkness. 4,6-Diamidino-2-phenylindole (1 μg mL^{-1}) was used to counterstain the nDNA. The sections were treated with 0.01% toluidine blue in PBS to diminish the autofluorescence of the tissue. Alternatively, a set of sections from similar treatments was stained with 0.1% aniline blue (Serva) in PBS (pH 9.2) for visualizing the Al-induced callose deposits.

Immunofluorescence Localization of F-Actin

The sections were dried overnight at room temperature, dewaxed in ethanol, rehydrated in an ethanol/PBS series, and allowed to stand in stabilizing buffer for 30 min. Afterward, the sections were treated for 10 min with absolute methanol at −20°C and transferred to stabilizing buffer for 30 min. Then they were incubated with mouse-monoclonal anti-actin antibody (clone C4) raised against chicken gizzard actin (ICN Biomedicals), diluted 1:200

in PBS for 90 min at room temperature. After a further rinse with stabilizing buffer, the actin antibody-conjugated sections were stained with fluorescein isothiocyanate-conjugated anti-mouse IgG raised in goat, diluted 1:100 in PBS for 60 min at room temperature. Sections were counterstained with 4,6-diamidino-2-phenylindole (1 μg mL^{-1}) followed by 0.01% toluidine blue in PBS to diminish the natural autofluorescence of root tissues.

Microscopy and Image Evaluation

We examined and evaluated the fluorescence of labeled sections, mounted on the anti-fade mountant (Baluška et al., 1992), using an Axiovert 405M inverted microscope (Zeiss) equipped with epifluorescence, a standard fluorescein isothiocyanate exciter, and barrier filters (BP 450-490, LP 520). We photographed the fluorescent images under similar exposure times (between the control and Al treatments to assess the Al-elicited differences in the fluorescence intensity) on Kodak T-Max 400 ASA films. All experiments were repeated at least twice, comprising 3 to 10 replicates. We analyzed at least five to six root apices from each experiment and documented the results.

The organization of MTs and actin MFs in cells of the control and experimentally treated root apices were systematically documented from the root cap junction to the end of the growth region, approximately 8-mm DFT. Most of the observations were of cells of the epidermis and of the two to three outermost cortex cell files (outer cortex) in the DTZ and in the middle part of the TZ, where we viewed major changes to the cytoskeleton (for additional details on zone specifications, see Sivaguru and Horst, 1998). However, the root-zone specifications of the nutrient solution-grown seedlings may vary from those of the plants grown in humid air (Ishikawa and Evans, 1993). Hence, we cannot exclude overlapping from the DTZ to the proximal part of the meristematic zone.

Electrophysiology

A standard electrophysiological setup was used (Felle, 1981). Micropipettes were pulled on a Getra instrument (vertical) from borosilicate tubing with solid filaments (Hilgenberg, Malsfeld, Germany) and filled by capillary displacement with 0.5 M KCl. Tip diameters were 0.4 to 0.5 μm. The micropipettes were connected through an Ag/AgCl half-cell to a high-impedance amplifier (FD 223, World Precision Instruments, Sarasota, FL). Signals were recorded on a pen chart (L 2200, Linseis, Selb, Germany). Measurements were carried out under constant perfusion in a Plexiglas chamber, which was open on both sides to allow the horizontal approach of the micropipette(s) at room temperature. Following a 10- to 20-min equilibration in the nutrient solution, which was supplemented with 200 μM $CaCl_2$ and 200 μM KCl, impalements were made in the outermost cortical cells 1 to 3 mm behind the root tip, at 200-μm intervals. As soon as the membrane potential was stable for at least 5 min, the chamber was perfused with the Al test solution. The kinetics given are representative of at least 11 tests carried out on individual roots.

RESULTS

Effects of Al on Root Growth

Al (90 μM monomeric Al) exerted significant inhibition of the root-elongation rate after 1 h of treatment (about 20% inhibition) in the Al-sensitive maize cv Lixis (Fig. 1). Prolonged Al treatment led to increasingly severe inhibition of root elongation (50% and 60% after 2 and 6 h, respectively).

Effects of Short-Term (1-h) Al Treatment on MTs

One hour of Al treatment proved to have dramatic effects on MTs, but this early impact was limited to cells of the outermost cortical cell file located within the DTZ (Fig. 2, A and B). These unique cells were devoid of any MTs, whereas the epidermis cells still displayed distinct tubulin fluorescence (Fig. 2B). Figure 2C is the DIC image of Figure 2B and shows the integrity of the cells.

In contrast to the cell periphery of the DTZ region, cells of other root regions showed the same MT cytoskeleton as found in the control roots (which is almost identical with data previously published; see e.g. Baluška et al. [1992]). In this study we are documenting this situation for cells of the elongation region, focusing again on the epidermis and the outer cortex. Dense, transversally running arrays of CMTs are the most typical features of any elongating root cell, and Figure 2D documents this for the epidermis of control roots. Short-term (1-h) Al treatment had no effect on CMTs in cells of both of the epidermis and outer cortex, which displayed dense arrays oriented transversally with respect to the root growth axis (Fig. 2E).

An effect of the short-term Al treatment was also found in meristematic cells, in which endoplasmic perinuclear MTs obtained an extremely bright appearance (Fig. 2F). This phenomenon, indicating an increased tubulin polymerization in dividing cells, was consistently recorded in-all dividing cells and culminated in some abnormalities in

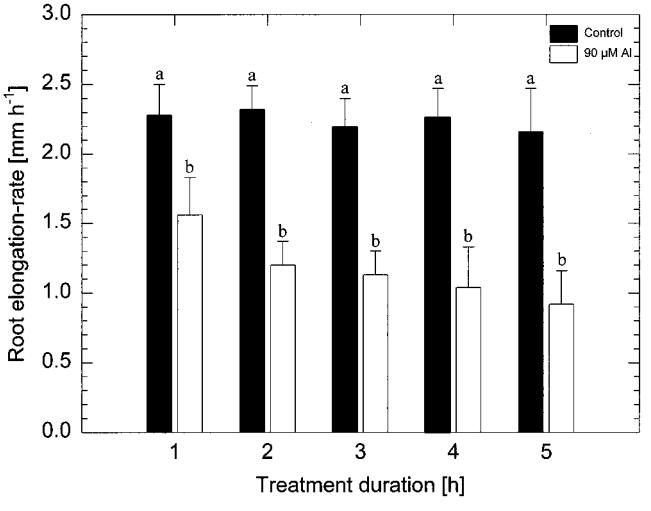

Figure 1. Effect of 90 μM monomeric Al on root-elongation rate of the Al-sensitive maize cv Lixis treated for 1 to 5 h. Values are means of five independent replicates. Means followed by the same letter do not differ significantly at $P < 0.05$ (Tukey's test).

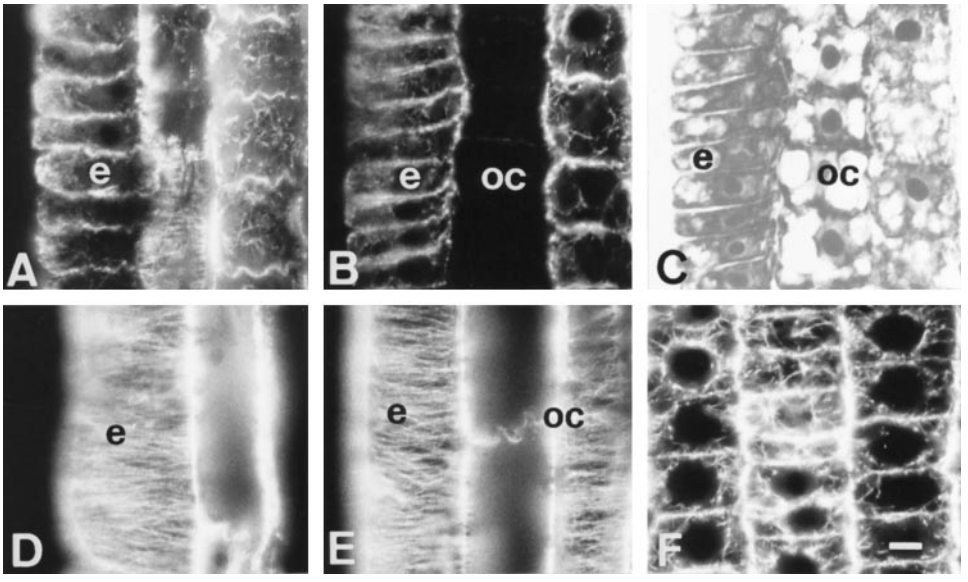

Figure 2. Effects of short-term Al treatment (90 μM, 1 h) on MTs in cells of the DTZ (A, B, and C) and of the elongation region (D and E). A and D, Control. C is the DIC image of B. The most sensitive cells with respect to Al effects on the MT cytoskeleton proved to be the outermost cortical cells of the DTZ, as these lost all of their MTs after 1 h of Al treatment (B). In contrast, no effects on MTs were found in the elongation zone (D and E). Extremely dense endoplasmic MTs were induced by 1 h of Al in the apical meristem (F). e, Epidermis; oc, outer cortex. Bar = 8 μm for A to E and 6 μm for F.

phragmoplast orientations and division plane alignments after long-term Al treatments (data not shown).

Effects of Medium-Term (6-h) Al Treatment on MTs

The epidermis and outer cortex cells of the DTZ progressively increased their lesions in the MT cytoskeleton during further exposures to Al. Both of these tissues were almost devoid of any CMTs after 6 h of Al treatment (Fig. 3A; for corresponding DIC image see Fig. 3B).

Contrasting behavior was found in the epidermis and outer cortex cells of the elongation region where CMT arrays still maintained dense, transversally oriented arrays (see Fig. 3C for epidermis cells and Fig. 3D for outer cortex cells) comparable to those present in control root cells (Fig. 2D; see also Baluška et al., 1992). Nevertheless, more deeply localized cells of the outer cortex (the third cell file from the epidermis) often exhibited an increased randomization of their CMT arrays (see the middle part of Fig. 3D). This phenomenon was especially prominent in cells of the

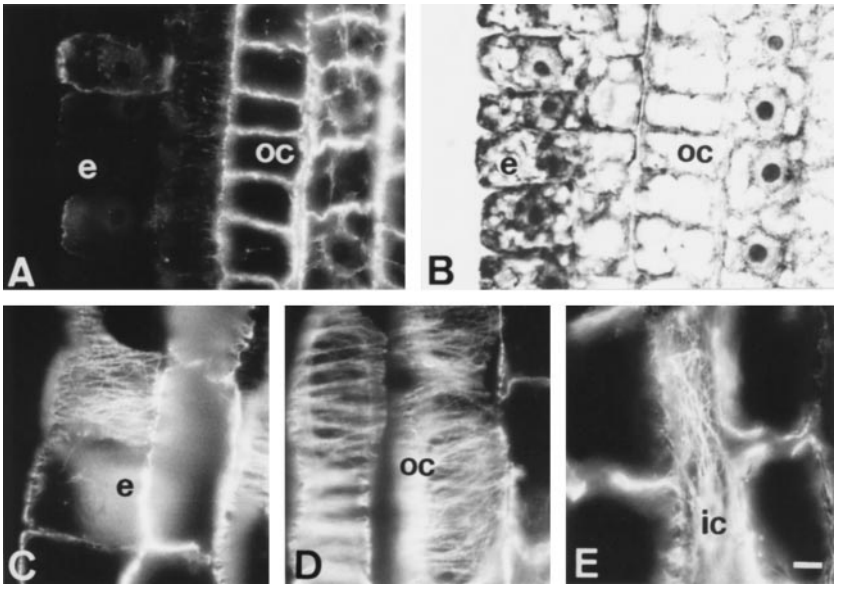

Figure 3. Effects of medium-term Al treatment (90 μM, 6 h) on MTs of cells in the DTZ (A and B) and in the elongation zone (C, D, and E). In the DTZ the outermost cortical and epidermal cells are devoid of MTs (A) whereas cells of the elongation region show dense arrays of transverse CMTs (C and D). In some inner cortex cells, longitudinal arrangement of CMTs was found (E). e, Epidermis; oc, outer cortex; ic, inner cortex. Bar = 10 μm.

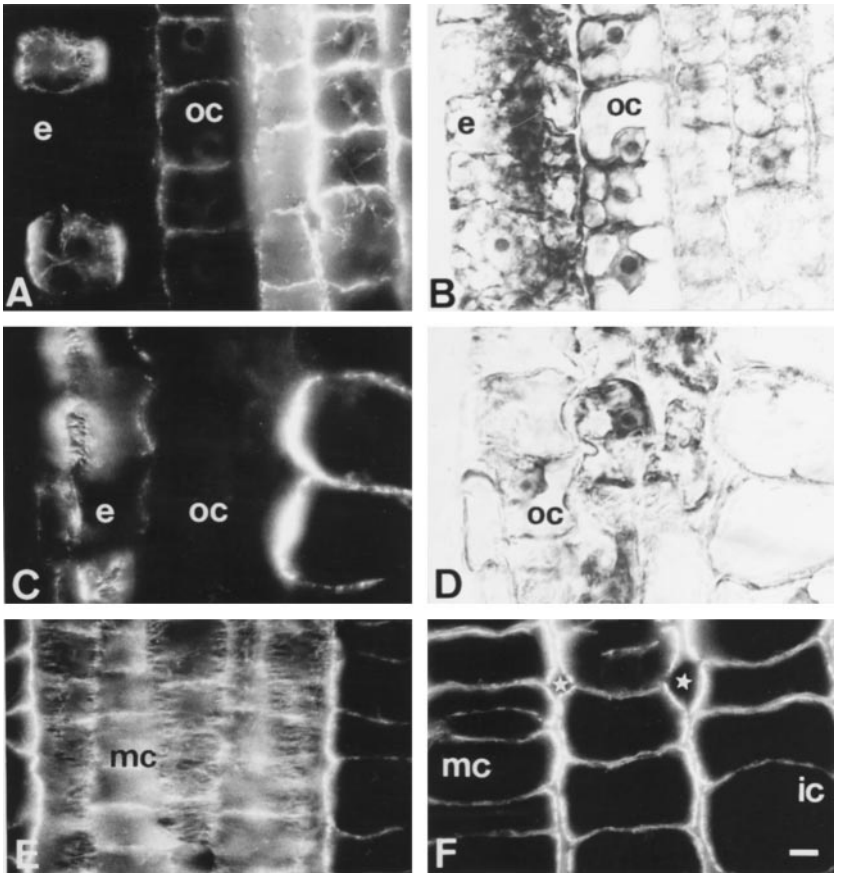

Figure 4. Effects of long-term Al treatment (90 μM, 12 h) on MTs and cell shapes in DTZ (A and B) and proximal (C and D) part of the TZ. B and D are DIC images of A and C. Note that epidermal and outer cortex cells are already distorted in the proximal part of the TZ (C and D), whereas middle cortex cells are abnormally expanded (F). Note the presence of unusually large intercellular spaces (stars in F). Although most cells of the middle cortex have disoriented CMTs, some cells still show dense transversal arrays (E). e, Epidermis; oc, outer cortex; ic, inner cortex; mc, middle cortex. Bar = 8 μm.

inner cortex where even longitudinal arrays of CMTs were found (Fig. 3E).

Effects of Long-Term (12-h) Al Treatment on MTs

After 12 h of Al treatment the most dramatic lesions to the MT cytoskeleton still encountered the epidermis and outer cortex cells, but they progressively spread from the DTZ (Fig. 4, A and B) to the proximal part of the TZ (Fig. 4, C and D). The DIC image of Figure 4C revealed that in the proximal part of TZ first degeneration features occurred in tissues of the root periphery (Fig. 4D).

The more internal cortex tissues showed rather dense randomized CMT arrays (not shown) although many middle and inner cortex cells still displayed well-ordered dense arrays of CMTs (Fig. 4E). Despite this, the overall cellular morphology of the middle and inner cortex was changed throughout the TZ and roundish shapes with large intercellular spaces was the characteristic feature of root apices treated with Al for 12 h (Fig. 4F).

Comparable Effects of Al and NPA

Periclinal divisions in meristematic cortical cells induced by NPA (Fig. 5A) could be mimicked by Al (Fig. 5B), both treatments lasting 6 h. These divisions were preceded by unusual, vertical preprophase bands (data not shown).

Effects of Short-Term (1-h) and Long-Term (6-h) Al Treatments on Actin MFs

Short-term (1-h) Al treatment (Fig. 6, D and F) induced alterations to the actin MF polymerization, as evidenced from decreased amounts of F-actin and increased actin fluorescence in Al-treated root apices. These alterations were comparable to those shown after 6 h of Al treatment (Fig. 6B). The most prominent effect was observed in the

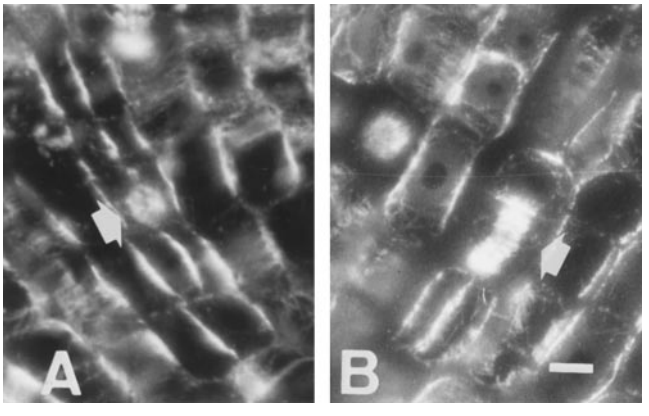

Figure 5. Induction of periclinal divisions in meristematic outer cortex by 10 μM NPA (A) and 90 μM Al (B), both supplied for 6 h. Bar = 8 μm.

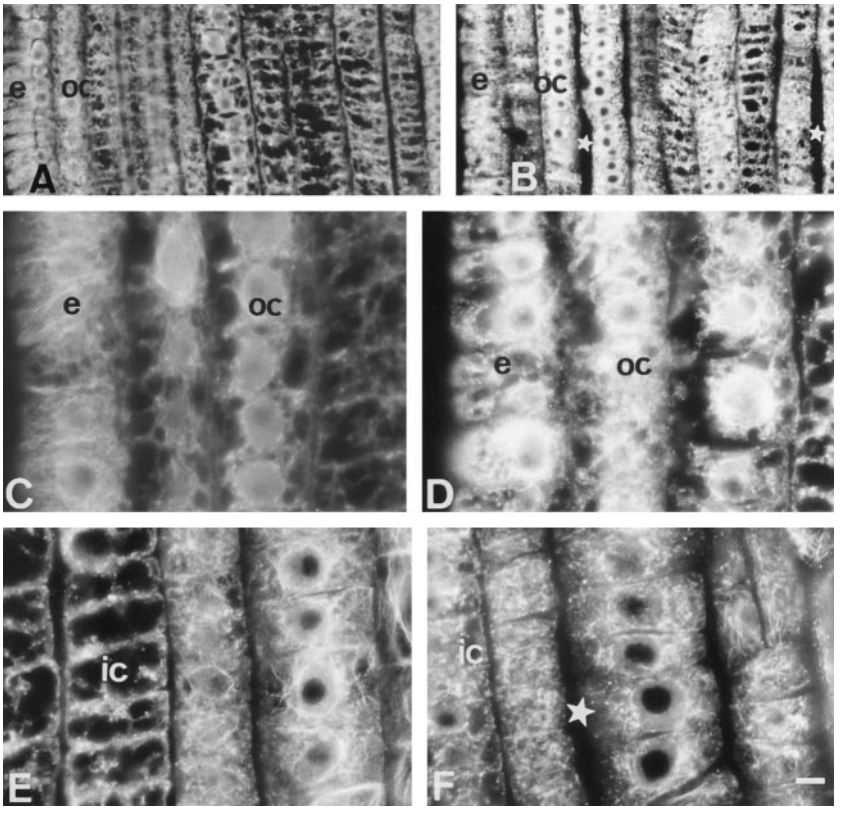

Figure 6. Effects of Al (90 μM) treatment on the actin MFs in apical root cells of an Al-sensitive maize cv Lixis. All images are from the DTZ region of the root apex. Comparable regions of control (A, C, and E) and 6-h (B) or 1-h (D and F) Al-treated root apices. Note the more prominent actin fluorescence and absence of filamentous actin in epidermal and outer cortex cells after Al treatments (B and D) when compared with their respective controls (A and C). Al-induced fragmentation or altered polymerization of actin MFs transforming almost all filamentous actin of inner cortex cells into actin-positive dots or F-actin fragments (F, compare the comparable control position, E). Note increased intercellular spaces in Al-treated root apices (stars in B and F). All root apices are facing the bottom of this figure. Bar = 16 μm (A and B) or 7 μm (all others). e, Epidermis; oc, outer cortex; ic, inner cortex.

DTZ (Fig. 6, compare A, C, and E with B, D, and F) and the middle part of the TZ (not shown). Al-induced fragmentation and/or altered actin polymerization enhanced the actin fluorescence in the epidermal and outer cortex cells (Fig. 6, compare A with B). Although our control images (Fig. 6E) show such actin-positive dots, an effect we attribute to low pH treatments, the Al-induced actin-positive dots or fragmented F-actin filaments were much more intense after 1 h of Al treatment (Fig. 6F). The outermost cortex cell layers usually have less distinct actin-positive dots but their actin fluorescence was more prominently increased by Al when compared with the more inner layers of the cortex (Fig. 6, compare D with F). This suggests that the formation of actin-positive dots was a less severe or indirect effect of Al compared with the direct severe effect of Al on the epidermal and outermost cortex cell layers of the same root apex. Pertinent with this, the metaxylem cells of DTZ also contained large amounts of actin-positive dots but cells of the stele periphery still showed thick bundles of actin MFs (data not shown).

Tissue-Specific Callose Formation

Images of Al-induced (90 μM, 1 h) callose deposits along the whole root apex indicate that callose formation was restricted only to the epidermis and outer cortex cells (Fig. 7). Along the entire root growth region, the intensity of callose deposition was highest in the outer cortex cells located within the DTZ (Fig. 7B), but it was also prominent in the outer cortex cells of the apical part of the elongation region (Fig. 7A) and the root tip near the quiescent center (Fig. 7C).

Al-Induced Changes to PM Potential

Upon the addition of 90 μM Al to the intact maize roots the membrane potential depolarized instantaneously by 55 $\pm$ 12 mV when impaled at 1.8-mm DFT (Fig. 8, a), but only by 15 $\pm$ 5 mV when impaled at 2.8 mm (Fig. 8, b).

DISCUSSION

Using the Al-sensitive maize cv Lixis, we demonstrate here that the root cytoskeleton shows the most prominent Al-induced alterations within cells of the distal part of the transition zone (DTZ) of maize root apices. Both MTs and actin MFs cytoskeleton were affected preferentially in cells of the DTZ. The relevance of the DTZ to the Al toxicity was further supported by the Al-induced callose formation (Fig. 7B) and the higher PM depolarization (Fig. 8) in this root zone.

Short-term Al treatment (1 h) was sufficient to produce profound disintegration of MTs in cells of the outermost cortex file. This dramatic lesion to the MT cytoskeleton was limited to cells of the DTZ, which was previously characterized as the most sensitive maize root region with respect to Al toxicity (Sivaguru and Horst, 1998). The most sensitive DTZ cells of the outermost cortex file showed complete depolymerization of all of their MTs after 1 h of Al treatment. This lesion became even more dramatic, expanding

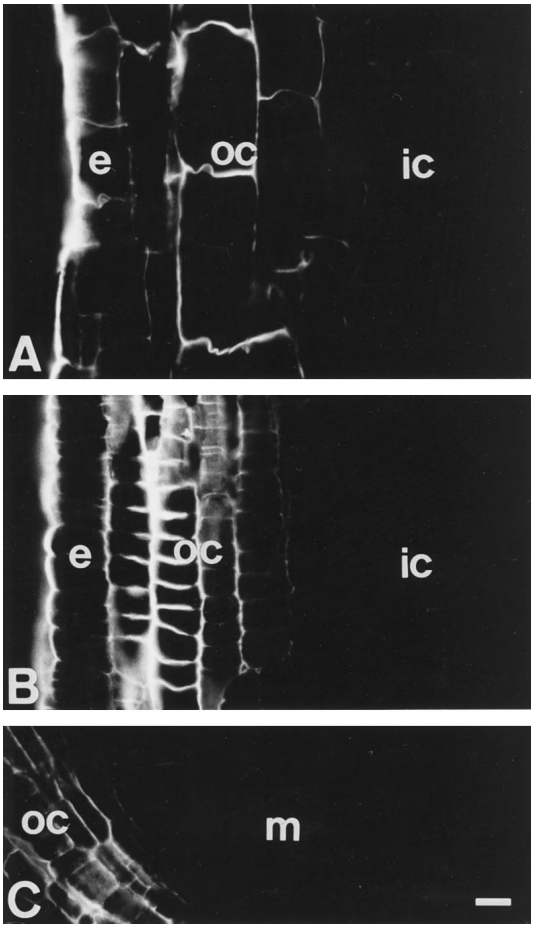

Figure 7. Al- (90 μM, 6 h) induced callose deposits in cells within the elongation zone (A). Cells of the DTZ accumulated the highest amounts of callose (B). Low amounts of callose were found in the outer cortex cells behind the quiescent center (C). The callose formation was restricted to the epidermis (e) and outer cortex (oc) cells throughout the root apex. All root apices are facing the bottom of this figure. ic, Inner cortex; m, meristem. Bar = 23 μm.

to most of the epidermis cells and to many root periphery cells of the proximal part of the TZ, after longer exposures of root apices to Al. For instance, after 12 h of Al treatment, most of the cells of the epidermis and the two outermost cortex files were depleted in their MT cytoskeleton. In contrast, cells within the meristem and elongation region retained their characteristic MT arrays, which appeared even more abundant and extensively bundled. Similar tissue-specific disintegration of MTs in maize root apices was also reported after high ethylene treatment when cells of the inner cortex lost their MTs, whereas outer cortex cells were rather resistant to ethylene (Baluška et al., 1993b). However, high auxin treatment temporarily depolymerized the MTs in all of the root cells (Baluška et al., 1996a). Although most of the elongating cortex cells preserved their transverse MT arrays, some inner cortex cells acquired randomly arranged CMTs after 1 h of Al treatment, and this feature became even more prominent after 6 and 12 h of Al treatment, when longitudinally arranged CMT arrays appeared in some inner cortex cells (see also Blancaflor et al., 1998). This confirms that the two to three outermost cortical layers, representing the outer cortex, are unique tissues, differing in many aspects from cells of the middle and inner cortex (Baluška et al., 1993a).

Our study confirms the findings of Blancaflor et al. (1998) that MTs of elongating cells are relatively insensitive to Al (at least as can be inferred from static immunofluorescence images) during the first 3 h of the Al exposure. However, focusing on the elongation zone, Blancaflor et al. (1998) missed those critical cells of the epidermis and outer cortex in the DTZ, which initiated degeneration of peripheral tissue domains in less than 3 h. Al-mediated alterations to the MT cytoskeleton and to the organization of the maize root apex can be mimicked by auxin over-supplies (Blancaflor and Hasenstein, 1995a; Baluška et al., 1996b) and by auxin-transport inhibitors (Kerk and Feldman, 1994; Ruegger et al., 1997; this study). For instance, as already mentioned, high auxin levels induced temporary depolymerization of MTs. Another typical auxin-induced response of the MT cytoskeleton was a rearrangement of CMTs, which typically changed from transverse to random and longitudinal arrays (Blancaflor and Hasenstein, 1995a; Baluška et al., 1996b). Imbalances to endogenous auxin levels could be relevant for morphological disorders, such as the newly induced, periclinal divisions and subapical root swellings (Kerk and Feldman, 1994; Ruegger et al., 1997; Blancaflor et al., 1998). Al-induced inhibition of root growth, associated with progressively increased growth anisotropy, might be expected to involve disruption of putative auxin-cytoskeleton interactions (for review, see Shibaoka, 1994; Baluška et al., 1998). This is especially valid for cells of the TZ, which are unique in their responses to external auxin (Ishikawa and Evans, 1993, 1995). Although a direct effect of Al on the basipetal transport of [^{3}H]IAA was demonstrated by Hasenstein and Evans (1988), and although the transport was localized within the outer cortex (Tsurumi and Ohwaki, 1978), no follow-up work has been presented on this important aspect of Al rhizotoxicity.

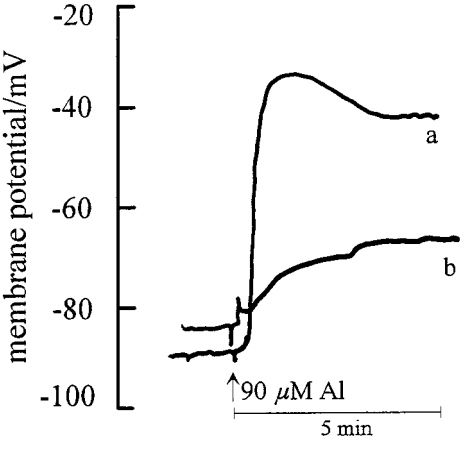

Figure 8. Effect of 90 μM Al supply on the PM potentials in the outer cortex cells of an Al-sensitive maize cv Lixis root apex. Impalement was at 1.8 mm (a) and at 2.8 mm (b) DFT (n = 11). Data are representative of single recordings.

Increased cytosolic Ca^{2+} and modification of the PM are known to be crucial factors for the induction of callose synthesis (Kauss et al., 1990). In agreement with this, Al induced a higher callose content (Fig. 7B; see also Sivaguru and Horst, 1998) and higher PM depolarization in the outer cortex cells of the DTZ, compared with the cells of more basal root zones (Fig. 8). Similar effects of Al on the electrical properties of the PM were also reported for characean cells by Takabatake and Shimmen (1997). These authors concluded that the PM represents the primary target of Al toxicity. On the other hand, Papernik and Kochian (1997) described higher PM depolarization only in the Al-tolerant cultivar in wheat root apices, which was correlated to organic acid exudation. Binding and/or interaction of Al with the PM may lead to alterations in the CMT arrays underlying the PM and, in the most affected cells, even to the failure to maintain its presence. Cells in the inner cortex, which are probably not exposed directly to Al, showed only alterations to the distribution of CMT; there was no Al-induced callose formation. The very rapid effect of Al on the PM potential in the DTZ, but not the elongation zone, might indicate that this depolarization triggers a cascade of events leading to the effect on the cytoskeleton and to the callose formation measured after 1 h, but is probably initiated much earlier. This will be a focus of our future studies.

The present observations suggest that, in addition to the cell wall structure (Le Van et al., 1994), Al especially affects the integrity of the PM and the cytoskeletal organization in cells located specifically within the DTZ. Although the cytoskeleton/PM/cell wall structural continuum is not yet fully established for plant cells (Wyatt and Carpita, 1993; Miller et al., 1997), it is almost accepted that such an interconnected superstructure does exist at the plant-cell periphery. Al is known to bind strongly to the cell wall, to the PM, and to many Ca^{2+}, Mg^{2+}, and negatively charged binding sites in the apoplast, and to enter the cytoplasm (for review, see Horst, 1995; Kochian, 1995). If we accept the existence of the cytoskeleton/PM/cell wall continuum in the maize root apex, Al does not necessarily need to enter the cytoplasm to alter cytoskeletal dynamics. Such a structural continuum means that alterations to any extracellular component of this continuum may have direct impacts on the underlying cytoskeletal structures, which are bound to the cytoplasmic face of the PM.

In the presence of Al, the overall increase in the intensity of actin fluorescence indicates that the actin MF polymerization might be altered upon exposure to Al. In particular, the cells of the epidermis and outer cortex of the DTZ showed an increased actin MF fluorescence due to fragmentation or altered polymerization of filamentous actin, which corresponded well to Al-mediated alterations of CMT arrays. Inner layers of cortex cells were not characterized by such alteration, but have fragmented actin or actin-positive dots. Grabski and Schindler (1995) found that Al induced an increase in the stability/rigor within the actin MF network, with no gross change in the appearance in a concentration-dependent manner, which was in agreement with our observation in outer stele cells (unusually thick actin MFs [data not shown]). However, it is difficult to reconcile the direct effect of Al on the metaxylem and middle cortex cells (Fig. 6F) during the short-term Al treatments, which showed disintegrated actin MFs with numerous actin-positive dots. Rather, this finding indicates that Al binding to cells of the epidermis and outer cortex may simultaneously induce the transfer of putative signals, which alters the cytoskeletal structures of more inner cell layers. Recently, for instance, Schofield et al. (1998) demonstrated the slow/restricted radial Al transport in onion roots. This suggests that cells of individual tissues differ with respect to Al impacts on their actin cytoskeleton.

As discussed above, it is possible that rapid Al-induced changes to cytosolic Ca^{2+} may mediate cytoskeletal disorders. Although many environmental signals including Al induced an increase in the cytosolic Ca^{2+} levels (Lindberg and Strid, 1997), the recent evidence argues for Al-induced decreases in the levels of cytosolic Ca^{2+} (Jones et al., 1998). An increase in the tension of actin occurred when the cytosolic Ca^{2+} levels were altered by the signaling substances, including auxin in soybean cells (Grabski and Schindler, 1996). The latest work from their laboratory revealed that Al affects actin MFs via involvement of Ca^{2+}-regulated kinases and phosphatases (Grabski et al., 1998). In line with this, inhibitors of protein kinases and phoshatases (e.g. calyculin A and staurosporine) were shown to disorganize the MT-cytoskeleton, specifically the CMTs, which impaired root elongation through induction of radial growth and swelling in Arabidopsis (Baskin and Wilson, 1997). In comparison with plant systems, direct Al interaction with the actin MFs were studied more profoundly in mammalian systems such as HeLa cells, where Al interaction with actin MFs and subsequent protrusions in the PM were described (Radhakrishna et al., 1996, and refs. therein). Recently, Jones and Kochian (1995) found that Al specifically inhibits the phospholipase C activity in wheat root cells, and they proposed a link to the inositol 1,4,5-trisphophate signal transduction pathway. This particular finding suggests that the Al action in plant and animal cells (e.g. McDonald and Mamrack, 1995) may be basically similar. Accordingly, in neuroblastoma cells, phosphotidylinositol-4,5-diphosphate (PIP_2)-specific phospholipase C was characterized as a potential Al-interaction site through guanine nucleotide-binding, protein-coupled transmembrane signaling (Haug et al., 1994). Later, Jones and Kochian (1995) provided evidence of a direct Al-mediated inhibition of phospholipase C and hypothesized that the phosphoinositide-signaling pathway might be the initial target of Al. In accordance with this hypothesis, components of the actin-based cytoskeleton were found to directly interact with phospholipase C (Huang et al., 1998), a crucial enzyme in the plant phosphoinositide signaling cascade and even to regulate its activity (Drøbak et al., 1994).

The data presented here provide circumstantial evidence that in an Al-sensitive maize cultivar, Al-induced inhibition of root elongation involves inherent Al/PM/cytoskeleton interactions especially in the DTZ of the root apex. Although the Al-induced stabilization or rigidification of MTs in the elongation zone observed by Blancaflor et al. (1998) after 3 h could explain the inhibition of elongation

rate, the alterations detected here after 1 h in DTZ may be decisive and more closely linked to Al-induced growth inhibition within this time frame (an observation that requires further attention). The specialized cells of this zone, which are undergoing a preparatory phase for the rapid cell elongation (Baluška et al., 1996b), are extremely sensitive to Al. Whether Al affects the organization of cytoskeletal elements by modifying protein phosphorylation and the cell wall structures connected to it and whether it causes disturbances of the Ca^{2+} homeostasis and/or phytohormonal signaling needs to be clarified in future studies.

ACKNOWLEDGMENTS

M.S. and W.J.H. are grateful to Prof. P. Schopfer, Institute of Biology, University of Freiburg, Germany, for introducing M.S. to the field of cytoskeletons and to Dr. G. Grunewaldt, Institute of Plant Pathology and Plant Protection, and Dr. C. Weigle, Institute of Animal Sciences (TiHo), University of Hannover, Germany, for their excellent technical advice. We would also like to thank Prof. H. Matsumoto, Research Institute for Bioresources, Okayama University, Japan, for providing materials for additional experiments, and Katsuaki Takechi for help with Adobe Photoshop 4.0J, as well as the anonymous reviewers for their critical suggestions regarding presentation and discussion of the results.

Received June 26, 1998; accepted December 4, 1998.

LITERATURE CITED

Alfano F, Russell A, Gambardella R, Duckett JG (1993) The actin cytoskeleton of the liverwort *Riccia fluitans*: effects of cytochalasin B and aluminium ions on rhizoid tip growth. J Plant Physiol **142:** 569–574

Baluška F, Barlow PW, Hauskrecht M, Kubica Š, Parker JS, Volkmann D (1995) Microtubule arrays in maize root cells: interplay between the cytoskeleton, nuclear organization and postmitotic cellular growth patterns. New Phytol **130:** 177–192

Baluška F, Barlow PW, Volkmann D (1996a) Complete disintegration of the microtubular cytoskeleton precedes auxin-mediated reconstruction in postmitotic maize root cells. Plant Cell Physiol **37:** 1013–1021

Baluška F, Brailsford RW, Hauskrecht M, Jackson MB, Barlow PW (1993a) Cellular dimorphism in the maize root cortex: involvement of microtubules, ethylene and gibberelin in the differentiation of cellular behaviour in postmitotic growth zones. Bot Acta **106:** 394–403

Baluška F, Hasenstein KH (1997) Root cytoskeleton: its role in perception of and response to gravity. Planta **203:** S-69–78

Baluška F, Hauskrecht M, Kubica Š (1990) Postmitotic 'isodiametric' cell growth in the maize root apex. Planta **181:** 269–274

Baluška F, Parker JS, Barlow PW (1992) Specific patterns of cortical and endoplasmic microtubules as associated with cell growth and tissue differentiation in roots of maize (*Zea mays* L.). J Cell Sci **103:** 191–200

Baluška F, Parker JS, Barlow PW (1993b) A role for gibberellic acid in orienting microtubules and regulating cell growth polarity in the maize root cortex. Planta **191:** 149–157

Baluška F, Vitha S, Barlow PW, Volkmann D (1997) Rearrangements of F-actin arrays in growing cells of intact maize root apex tissues: a major developmental switch occurs in the postmitotic transition region. Eur J Cell Biol **72:** 113–121

Baluška F, Volkmann D, Barlow PW (1996b) Specialized zones of development in roots: view from the cellular level. Plant Physiol **112:** 3–4

Baluška F, Volkmann D, Barlow PW (1999) Hormone-cytoskeleton interactions. *In* KL Libbenga, M Hall, PJJ Hooykaas, eds, Biochemistry and Molecular Biology of Plant Hormones. Elsevier Publishing, Leiden, The Netherlands (in press)

Baluška F, Volkmann D, Hauskrecht M, Barlow PW (1996c) Root cap mucilage and extracellular calcium as modulators of cellular growth in postmitotic growth zones of the maize root apex. Bot Acta **109:** 25–34

Barlow PW, Parker JS (1996) Microtubular cytoskeleton and root morphogenesis. Plant Soil **187:** 23–36

Baskin TI, Wilson JE (1997) Inhibitors of protein kinases and phosphatases alter root morphology and disorganize cortical microtubules. Plant Physiol **113:** 493–502

Blancaflor EB, Hasenstein KH (1993) Organization of microtubules in graviresponding corn roots. Planta **191:** 231–237

Blancaflor EB, Hasenstein KH (1995a) Time course and auxin sensitivity of cortical microtubule reorientation in maize roots. Protoplasma **185:** 72–82

Blancaflor EB, Hasenstein KH (1995b) Growth and microtubule orientation of maize roots subjected to osmotic stress. Int J Plant Sci **156:** 794–802

Blancaflor EB, Hasenstein KH (1997) The organization of the actin cytoskeleton in vertical and graviresponding primary root of maize. Plant Physiol **113:** 1147–1455

Blancaflor EB, Jones DL, Gilroy S (1998) Alterations in the cytoskeleton accompany aluminum-induced growth inhibition and morphological changes in primary roots of maize. Plant Physiol **118:** 159–172

Delhaize E, Ryan PR (1995) Aluminum toxicity and tolerance in plants. Plant Physiol **107:** 315–321

Drøbak BK, Watkins PAC, Valenta R, Dove S, Lloyd CW, Staiger CJ (1994) Inhibition of plant plasma membrane phosphoinositide phospholipase C by the actin-binding protein, profilin. Plant J **6:** 389–400

Felle HH (1981) A study of the current-voltage relationships of electrogenic active and passive membrane elements in *Riccia fluitans*. Biochim Biophys Acta **646:** 151–160

Grabski S, Arnoys E, Busch B, Schindler M (1998) Regulation of actin tension in plant cells by kinases and phosphatases. Plant Physiol **116:** 279–290

Grabski S, Schindler M (1995) Aluminum induces rigor within the actin network of soybean cells. Plant Physiol **108:** 897–901

Grabski S, Schindler M (1996) Auxins and cytokinins as antipodal modulators of elasticity within the actin network of plant cells. Plant Physiol **110:** 965–970

Hasenstein KH, Evans ML (1988) Effects of cations on hormone transport in primary roots of *Zea mays*. Plant Physiol **86:** 890–894

Haug A (1994) Molecular aspects of aluminum toxicity. Crit Rev Plant Sci **1:** 345–373

Haug A, Shi B, Vitorello V (1994) Aluminum interaction with phosphoinositide-associated signal transduction. Arch Toxicol **68:** 1–7

Horst WJ (1995) The role of the apoplast in aluminum toxicity and resistance of higher plants: a review. Z Pflanzenernaehr Bodenkd **158:** 419–428

Horst WJ, Püschel A-K, Schmohl N (1997) Induction of callose formation is a sensitive marker for genotypic aluminium sensitivity in maize. Plant Soil **192:** 23–30

Huang CH, Cote GG, Crain RC (1999) Phosphoinositide-specific phopholipase C in oat roots. Association with actin cytoskeleton. Plant Physiol (in press)

Ishikawa H, Evans ML (1993) The role of the distal elongation zone in the response of maize roots to auxin and gravity. Plant Physiol **102:** 1203–1210

Ishikawa H, Evans ML (1995) Specialized zones of development in roots. Plant Physiol **109:** 725–727

Jones DL, Kochian LV (1995) Aluminium inhibition of the inositol 1,4,5-triphosphate signal transduction pathway in wheat roots: a role in aluminium toxicity? Plant Cell **7:** 1913–1922

Jones DL, Kochian LV, Gilroy S (1998) Aluminum induces a decrease in cytosolic calcium concentration in BY-2 tobacco cell cultures. Plant Physiol **116:** 81–89

Jones DL, Shaff JE, Kochian LV (1995) Role of calcium and other ions in directing root hair tip growth in *Limnobium stoloniferum*. I. Inhibition of tip growth by aluminum. Planta **197:** 672–680

Kauss H, Waldmann T, Quader H (1990) Ca^{2+} as a signal in the induction of callose synthesis. *In* R Ranjeva, AM Boudet, eds, Signal Perception and Transduction in Higher Plants. Springer-Verlag, Berlin, pp 117–131

Kerk N, Feldman, L (1994) The quiescent center in roots of maize: initiation, maintenance and role in organization of the root apical meristem. Protoplasma **183:** 100–106

Kerven GL, Edwards DG, Asher CJ, Hallman PS, Kokot S (1989) Aluminium determination in soil solution. II. Short term calorimetric procedures for the measurement of inorganic monomeric aluminium in the presence of organic acid ligands. Aust J Soil Res **27:** 91–102

Kinraide TB, Ryan PR, Kochian LV (1992) Interaction effects of Al^{3+}, H^+, and other cations on root elongation considered in terms of cell-surface electrical potential. Plant Physiol **99:** 1461–1468

Kochian LV (1995) Cellular mechanisms of aluminum toxicity and resistance in plants. Annu Rev Plant Physiol Plant Mol Biol **46:** 237–260

Lazof DB, Goldsmith JG, Rufty TW, Linton RW (1994) Rapid uptake of aluminum into cells of intact soybean root tips. A microanalytical study using secondary ion mass spectroscopy. Plant Physiol **106:** 1107–1114

Le Van H, Kuraishi S, Sakurai N (1994) Aluminium-induced rapid root inhibition and changes in cell-wall components of squash seedlings. Plant Physiol **106:** 971–976

Lindberg S, Strid H (1997) Aluminium induces rapid changes in cytosolic pH and free calcium and potassium concentrations in root protoplasts of wheat (*Triticum aestivum*). Physiol Plant **99:** 405–414

Llugany M, Massot N, Wissemeier AH, Poschenrieder C, Horst WJ, Barcelo J (1994) Aluminum tolerance of maize cultivars as assessed by callose production and root elongation. Z Pflanzenernaehr Bodenkd **157:** 447–451

MacDonald TL, Humphreys WG, Martin RB (1987) Promotion of tubulin assembly by aluminum ion in vitro. Science **236:** 183–186

McDonald LJ, Mamrack MD (1995) Phosphoinositide hydrolysis by phospholipase C modulated by multivalent cations La^{3+}, Al^{3+}, neomycin, polyamines and melittin. J Lipid Mediat Cell Signal **11:** 81–91

Miller D, Hable W, Gottwald J, Ellard-Ivey M, Demura T, Lomax T, Carpita N (1997) Connections: the hard wiring of the plant cell for perception, signaling, and response. Plant Cell **9:** 2105–2117

Papernik LA, Kochian LV (1997) Possible involvement of Al-induced electrical signals in Al tolerance in wheat. Plant Physiol **115:** 657–667

Radhakrishna H, Klausner RD, Donaldson JG (1996) Aluminum fluoride stimulates surface protrusions in cells over expressing the ARF6 GTPase. J Cell Biol **134:** 935–947

Rengel Z (1996) Uptake of aluminium by plant cells. New Phytol **134:** 389–406

Ruegger M, Dewey E, Hobbie L, Brown D, Bernasconi P, Turner J, Muday G, Estelle M (1997) Reduced naphthylphthalamic acid binding in the *tir3* mutant of Arabidopsis is associated with a reduction in polar auxin transport and diverse morphological defects. Plant Cell **9:** 745–757

Ryan PR, Di Tomaso JM, Kochian LV (1993) Aluminium toxicity in roots: an investigation of spatial sensitivity and the role of the root cap. J Exp Bot **44:** 437–446

Sasaki M, Yamamoto JM, Matsumoto H (1997) Aluminum inhibits growth and stability of cortical microtubules in wheat (*Triticum aestivum*) roots. Soil Sci Plant Nutr **43:** 469–472

Schofield RMS, Pallon J, Fiskesjö G, Karlsson G, Malmqvist KG (1998) Aluminum and calcium distribution patterns in aluminum-intoxicated roots of *Allium cepa* do not support the calcium-displacement hypothesis and indicate signal-mediated inhibition of root growth. Planta **205:** 175–180

Shibaoka H (1994) Plant hormone-induced changes in the orientation of cortical microtubules: alterations in the cross-linking between microtubules and the plasma membrane. Annu Rev Plant Physiol Mol Biol **45:** 527–544

Sivaguru M, Horst WJ (1998) The distal part of the transition zone is the most aluminum-sensitive apical root zone of maize. Plant Physiol **116:** 155–163

Takabatake R, Shimmen T (1997) Inhibition of electrogenesis by aluminum in characean cells. Plant Cell Physiol **38:** 1264–1271

Taylor GJ (1995) Overcoming barriers to understanding the cellular basis of aluminum resistance. Plant Soil **171:** 89–103

Tsurumi S, Ohwaki Y (1978) Transport of ^{14}C-labeled indoleacetic acid in *Vicia faba* root segments. Plant Cell Physiol **19:** 1195–1206

Wyatt SE, Carpita NC (1993) The plant cytoskeleton-cell wall continuum. Trends Cell Biol **3:** 413–417

Zhang G, Slaski JJ, Archambault DJ, Taylor GJ (1997) Alteration of plasma membrane lipids in aluminum-resistant and aluminum-sensitive wheat genotypes in response to aluminum stress. Physiol Plant **99:** 302–308